Performances of vector control of a Brushless Dual-Fed Induction Generator Incorporated in a wind energy conversion system with OTC-MPPT

Mohamed HAMIDAT, Katia KOUZI

University of Laghouat, Algeria

Laboratoire Matériaux, Systèmes Énergétiques, Energies Renouvelables et Gestion de l'Énergie (LMSEERGE)

mohamed.hamidat@lagh-univ.dz, k.kouzi@lagh-univ.dz

Abstract: Currently, the Brushless Dual-Fed Induction Machines (BDFIMs) are very often used in Wind Energy Conversion Systems (WECSs). The features of BDFIM are its high reliability due to its brushless operation, and the related lower capital and operational costs. This paper presents a field-oriented control algorithm for a Brushless Doubly-Fed Induction Generator (BDFIG). The proposed decoupled control is determined on the Power-Winding (PW) stator-flux frame and can be employed for controlling the rotation speed and its reactive power. In order, to avoid the use of an anemometer with speed sensors and to maximize wind energy extraction. Maximum Power Point Tracking (MPPT) based on Optimal Torque Control (OTC) is proposed. Several simulation results under different operating conditions are provided in order to prove the effectiveness of the proposed algorithm.

Keywords: Brushless Doubly-Fed Induction Machine (BDFIM), WECS, Vector Control, MPPT, Optimal Torque Control (OTC).

1. Introduction

High power wind turbines operate at variable speeds. The term variable speed refers to the fact that the speed of the turbine is independent of the frequency of the electrical network. These variable-speed systems were recently developed thanks to the evolution of power electronics, and they allow one to recover more energy, to reduce the costs of the mechanical system, to reduce noise and to improve the quality of the energy produced (Zhou et al., 1997).

Renewable energies are inexhaustible energies. Provided by the sun, the wind, the heat of the Earth, the waterfalls, their exploitation generates little or no waste and polluting emissions. These are the energies of the future. Today, they are underexploited in relation to their potential. Thus, renewable energies account for only 20% of global electricity consumption (Li & Pan, 2001).

Nowadays, efforts are all directed towards the development of renewable energy production, either locally or for large-scale production, depending on the potential of the site being exploited (Serhoud & Benattous, 2013). Several sources of renewable energy are being exploited and researched. Among these sources is wind energy (Eltamaly & Farh, 2013). The installation of high-power wind generators is being strongly considered in several countries.

The use of variable-speed wind turbines makes it possible to adjust the speed of variation for the generator. This is very useful for extracting the maximum power in the area where the MPPT algorithm is applied. For this operation, the aim is optimizing the power extracted from the machine by adapting the wind speed while maintaining a zero setting angle. For a wind turbine, MPPT can be defined as an algorithm capable of helping the WECS to extract the maximum electric power from the available kinetic energy of the wind. The output of the MPPT system is an optimum speed varying according to the wind speed captured (Bouras & Kouzi, 2017).

Various MPPT control techniques for WECS have been developed in the literature. These techniques can be classified into four control concepts based on the desired performance and measurement requirements, Perturbation and Observation (P&O) or Hill-Climbing Search (HCS), Power Signal Feedback (PSF) control, Tip Speed Ratio (TSR) control, and Optimal Torque control (OTC).

In recent years, there has been a lot of interest in the Brushless Doubly-Fed Induction Machine (BDFIM) due to its multiple advantages. Because its rotor can have a cage structure and given the

https://doi.org/10.33436/v32i2y202201

absence of brush-ring contact, the BDFIM is a robust machine. In addition, the possibility of controlling its speed and its power factor gives it, when used in wind systems, considerable advantages over conventional machines (Lobo, 2003).

Because of all these advantages, the BDFIM is considered a 3rd generation machine in the context of wind systems. Indeed, the cascade configuration of two Dual-Fed induction Machines (DFIM) can be considered the first practical realization of a dual-fed brushless machine. With the optimization of certain parameters such as size and robustness, and the integration of two windings in the same magnetic circuit of the stator. Thus, the BDFIM was acquired.

This paper is organized as follows. Section 1 as an introduction, Section 2 presents the modelling of the BDFIG. Section 3 deals with vector control of BDFIM in terms of active and reactive power of PW. Section 4 sets details of the MPPT with OTC of BDFIM. Section 5 presents the simulation results, while section 6 includes the conclusion and the proposals for future work.

This research focuses on the contribution of the proposed system to cost reduction, and solves many of the encountered problems regarding the implementation of wind speed sensors such as lack of space, and severe environment conditions by proposing the decoupled control of Brushless Doubly-Fed Induction generator incorporated in WECS with an OTC-MPPT scheme. The special merit of the OTC-MPPT-based generator lies in the fact that it is easy to implement, and it does not require any type of sensors.

2. Modelling of the conversion system

2.1. Modelling of the wind turbine

Before the description of the wind turbine first its principle of functioning should be outlined. The blades of the turbine are moved by the kinetic energy of wind and they transform this energy into mechanical power, which makes the turbine shift the direction of its rotation which in turn trains the generator, so first the mathematical model for defining the wind power should be built (Trejos-Grisales et al., 2014).

$$p_w = \frac{1}{2}\rho s v^3 \tag{1}$$

During its movement the wind turbine the wind loses some speed due to the flexible collisions with the blades. But behind the tower of the wind turbine the wind keeps moving and that means the wind turbine can't take all the available kinetic energy of wind but there is a limit known as the Betz limit or the power coefficient $c_p = {}^{16}\!/_{27}$. A lot of research was carried out in order to define the approximate formula for this coefficient but in this paper, the following expression of the power coefficient was chosen (Trejos-Grisales et al., 2014).

$$\left.\begin{aligned} c_p &= 0.5176\left(\frac{116}{\lambda_i} - 0.4\beta - 5\right)e^{\frac{21}{\lambda_i}} \\ \frac{1}{\lambda_i} &= \frac{1}{\lambda + 0.08\beta} - \frac{0.035}{\beta^2 + 1} \\ \lambda &= \frac{R\omega_m}{v} \\ \omega_m &= \frac{\Omega}{G} \end{aligned}\right\} \tag{2}$$

where R is the blade radius, β is the pitch angle of the blades, ω_m is the turbine slow speed shift and G is the gain of the gearbox. So the mechanical power and torque of the turbine under Betz limit can be expressed as: (Trejos-Grisales et al., 2014; Tria & Ben Attous, 2012).

$$P_T = \frac{1}{2} c_p \rho s v^3 \tag{3}$$

$$T_m = \frac{c_p \rho s v^3}{2\omega_m} \tag{4}$$

2.2. Dynamical model of the BDFIG

The BDFIG has two stators each with a different number of pole pairs. One of the windings is supplied with the grid voltage with the frequency fs and has pp pole pairs, namely the power winding (PW), the other is supplied with the voltage controlling the amplitude and the frequency fc and has pc pole pairs, namely control winding (CW). Since the windings have different pole pairs, they do not link directly, but they are coupled through the rotor that has n = pp + pc pole numbers (not pairs). In order to produce a co-operative torque with both windings in the rotor, the conditions pp, $\omega_r = \omega_p$ and pc, $\omega_r = \omega_c$ have to be kept, based on which (Perelmuter, 2016):

$$\omega_r = \frac{\omega_p - \omega_c}{p_p - p_c} \tag{5}$$

The equations of the BDFIG in the Park Transformation (d-q axes) are by Tir & Abdessemed (2014) and Rahab et al. (2017):

$$V_{dp} = R_p \cdot i_{dp} + \frac{d\psi_{dp}}{dt} - \omega_p \cdot \psi_{qp} \tag{6}$$

$$V_{qp} = R_p \cdot i_{qp} + \frac{d\psi_{qp}}{dt} + \omega_p \cdot \psi_{dp} \tag{7}$$

$$V_{dc} = R_c \cdot i_{dc} + \frac{d\psi_{dc}}{dt} - \omega_c \cdot \psi_{qc} \tag{8}$$

$$V_{qc} = R_c \cdot i_{qc} + \frac{d\psi_{qc}}{dt} + \omega_c \cdot \psi_{dc} \tag{9}$$

$$0 = R_r \cdot i_{dr} + \frac{d\psi_{dr}}{dt} - \omega_r \cdot \psi_{qr} \tag{10}$$

$$0 = R_r \cdot i_{qr} + \frac{d\psi_{qr}}{dt} + \omega_r \cdot \psi_{dr} \tag{11}$$

$$\omega_r = \omega_p - p_p \cdot \omega, \quad \omega_c = \omega_p - \left(p_p + p_c \right) \cdot \omega \tag{12}$$

Where ω is the rotor's mechanical angular speed.

The stator and rotor can be expressed as (Tir & Abdessemed, 2014; Perelmuter, 2016).

$$\psi_{dp} = L_p \cdot I_{dp} + M_p \cdot i_{dr} \tag{13}$$

$$\psi_{qp} = L_p \cdot I_{qp} + M_p \cdot i_{qr} \tag{14}$$

$$\psi_{dc} = L_c \cdot I_{dc} + M_c \cdot i_{dr} \tag{15}$$

$$\psi_{qc} = L_c \cdot I_{qc} + M_c \cdot i_{qr} \tag{16}$$

$$\psi_{dr} = L_r \cdot I_{dr} + M_p \cdot i_{dp} + M_c \cdot i_{dc} \tag{17}$$

$$\psi_{qr} = L_r . I_{qr} + M_p . i_{qp} + M_c . i_{qc} \tag{18}$$

The electromagnetic torque is calculated as (Lobo, 2003):

$$T_{em} = \frac{3}{2} P_p \left(\psi_{dp} \cdot i_{qp} - \psi_{qp} \cdot i_{dp} \right) + \frac{3}{2} P_p \left(\psi_{dc} \cdot i_{qc} - \psi_{qc} \cdot i_{dc} \right) \tag{19}$$

The active and reactive powers of the PW are defined as (Rahab et al., 2017):

$$P_p = \frac{3}{2} \left(V_{dp} \cdot i_{dp} + V_{qp} \cdot i_{qp} \right) \tag{20}$$

$$Q_p = \frac{3}{2} \left(V_{qp} \cdot i_{dp} - V_{dp} \cdot i_{qp} \right) \tag{21}$$

The three-phase voltages V_p and V_c are converted in the voltages V_{dp}, V_{qp}, V_{dc}, V_{qc} in the help of the Park transformation with angles $\theta_p = \int \omega_p dt$, and $\theta_c = \theta_p - \left(P_p + P_c \right) \theta_r$, where θ_r is the rotor angle.

3. Vector control of the BDFM

In order to be able to easily control the electricity production of the wind turbine, the principle of field-oriented control depends on the orientation of stator flux to the rotor, or to the air gap according to one of the two axes d or q. Two regulation paths are created as:

Reactive power control:

$$Q_P \rightarrow i_{dp^*} \rightarrow i_{dc^*} \rightarrow V_{dc^*}$$

Active power, electromagnetic torque or speed Control:

$$P_p \rightarrow i_{qp^*} \rightarrow i_{qc^*} \rightarrow V_{qc^*}$$

or

$$T_{em} \rightarrow i_{qp^*} \rightarrow i_{qc^*} \rightarrow V_{qc^*}$$

or

$$\Omega \rightarrow T_{em^*} \rightarrow i_{qp^*} \rightarrow i_{qc^*} \rightarrow V_{qc^*}$$

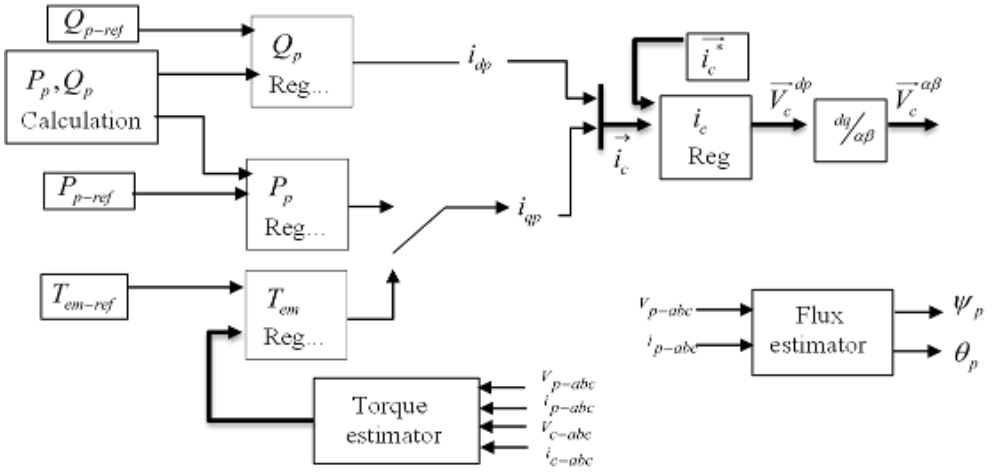

Figure 1. Vector control scheme of BDFIM using a Preportional Integral (PI) regulator

where i_{p-abc} and i_{c-abc} are 3 phase system current Components of the power winding current and the winding control current respectivly, i_c^* reference current.

3.1. The BDFG with a PW field oriented control

The PW flux orientation is $\psi_{dp} = \psi_p$ and $\psi_{qp} = 0$. So, the relation between the PW voltage and ψ_p is (Serhoud & Benattous, 2013):

$$\left.\begin{aligned} V_{dp} &= 0 \\ V_{qp} &= V_p = \omega_p \cdot \psi_p \end{aligned}\right\} \tag{22}$$

$$\left.\begin{aligned} \psi_{dp} &= L_p \cdot i_{dp} + M_p \cdot i_{dr} \\ 0 &= L_p \cdot i_{qp} + M_p \cdot i_{qr} \end{aligned}\right\} \tag{23}$$

3.2. Control of PW current

To find the ratio between the currents of the PW and the CW the flux of the PW was considered as a variable fixed by the supply voltage (independent variable). The relation between i_p and i_c can be expressed as (Lobo, 2003):

$$\frac{d_{idc}}{dt} = ax_{dc} \cdot i_{dp} + ay_{dc}\left(i_{qc}, i_{qp}, \psi_p\right) \tag{24}$$

$$\frac{d_{iqc}}{dt} = ax_{qc} \cdot i_{qp} + ay_{qc}\left(i_{dc}, i_{dp}, \psi_p\right) \tag{25}$$

where ax_{dc} and ax_{qc} represent the direct relation between i_p and i_c. If in the control diagram the terms, and $\frac{d_{idc}}{dt}, \frac{d_{iqc}}{dt}$ are current derivation. A ay_{dc} and ay_{qc} are added through the direct action "Feed forward". (Lobo, 2003):

$$ax_{dc} = \frac{R_r \cdot L_p}{M_c \cdot M_p} i_{dp} + \sigma_p \frac{L_r \cdot L_p}{M_c \cdot M_p} \frac{di_{dp}}{dt} \tag{26}$$

$$ax_{qc} = \frac{R_r \cdot L_p}{M_c \cdot M_p} i_{qp} + \sigma_p \frac{L_r \cdot L_p}{M_c \cdot M_p} \frac{di_{qp}}{dt} \tag{27}$$

$$ay_{dc} = \frac{R_r}{M_c \cdot M_p} \psi_p - \omega_p \frac{\sigma_p \cdot L_r \cdot L_p}{M_c \cdot M_p} i_{qp} + \omega_p \cdot i_{qc} \tag{28}$$

$$ay_{qc} = \omega_p \frac{\sigma_p \cdot L_r \cdot L_p}{M_c \cdot M_p} i_{dp} - \omega_p \cdot i_{dc} - \omega_p \frac{L_r}{M_c \cdot M_p} \psi_p \tag{29}$$

where $\sigma_p = 1 - \frac{M_p^{\ 2}}{L_p \cdot L_r}$

Figure 2 illustrates the suggested control algorithm which allows.to have CW reference current, in which it can be expressed as follows (Lobo, 2003):

$$i_p(s) = \frac{k_p}{\tau_p + 1} ax_c(s) \quad , \quad k_p = \frac{M_p \cdot M_c}{L_p \cdot R_r} \tag{30}$$

where $\tau_p = \frac{\sigma_p \cdot L_r}{R_r}$.

The term k_p is the PW controller parameter.

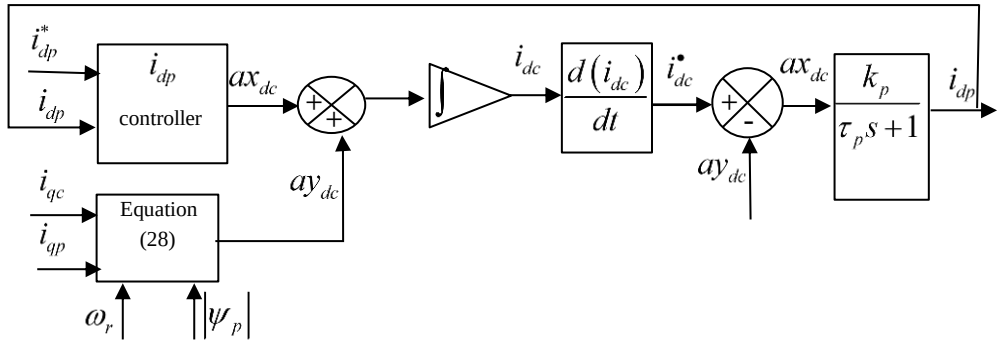

Figure 2. PW current control loop

where i^*_{dp} is the power winding reference current, and $i^{\bullet}_{dc}$ is the controle winding current.

3.3. Control of CW current

The voltage equation V_c based on i_c was obtained from equation (8) and (9) of the BDFIG.

$$V_{dc} = Vx_{dc} \cdot i_{dc} + Vy_{dc}\left(i_{qc}, i_{dp}, i_{qp}, \psi_p\right) \tag{31}$$

$$V_{dc} = Vx_q \cdot i_{qc} + Vy_{qc}\left(i_{dc}, i_{dp}, i_{qp}, \psi_p\right) \tag{32}$$

The transfer function is a first-order one (Lobo, 2003):

$$i_c(s) = \frac{k_c}{\tau_p s + 1} V_c(s) \ , \quad k_c = \frac{1}{R_c} \tag{33}$$

where $\tau_c = \dfrac{L_c - \dfrac{M_c^{\,2}}{L_r \cdot \sigma_p}}{R_c}$

The term k_c is the CW controller parameter.

3.4. Control of Torque

$$T_{em} = \frac{3}{2}\left(P_p + P_c\right) \cdot \psi_p \cdot i_{qp} \tag{34}$$

3.5. PW power control

The active and reactive powers of the PW manipulated within the machine depending only on the PW stator electric variable as it is expressed in equations (20) and (22). The PW is connected to the 50 Hz grid constant voltage, so the PW flux is maintained almost constant. In this way Q_p can be directly controlled by an adequate choice of i_{dp} since the active power can be directly controlled using the i_{qp} reference value (Lobo, 2003; Rahab et al., 2017).

$$\left.\begin{aligned} Q_p &= \frac{3}{2}\omega_p \cdot \psi_p i_{dp} \\ P_P &= \frac{3}{2}\omega_p \cdot \psi_p i_{qp} \end{aligned}\right\} \tag{35}$$

4. Maximum Power Point Tracking (MPPT) Control

The main objective of the MPPT method is to work the WECS around the power maximum. Several control blocks have been proposed to assure the MPPT such as MPPT with Optimal Torque Control (OTC), and PPT with Optimal Tip Speed Ratio (Aicha et al., 2019). This paper focuses on the OTC-MPPT scheme.

4.1. MPPT with OTC

The maximum power can also be obtained with optimal torque control according to equation (36):

$$T_{em}^{\,*} = K_{opt} \cdot \Omega^2_{mec} \tag{36}$$

and $K_{opt} = \dfrac{1}{2} \cdot \dfrac{\rho . C_{p-\max} \cdot R^5}{G^3 \cdot \lambda^3}$ (37)

Figure 3 illustrates the principle of MPPT with OTC.

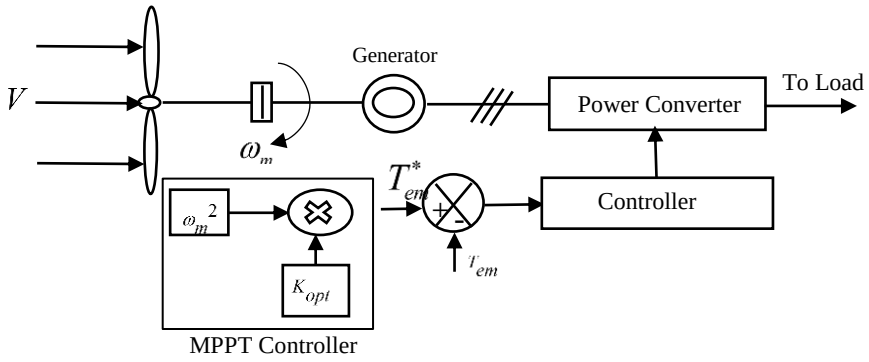

Figure 3. MPPT with optimal torque control of wind turbines

where Ω_{mec} is measured and employed in order to achieve torque reference T_{em}^*. Through the feedback control, the T_{em} will be equal to its reference T_{em}^* in steady state, and the MPPT is realized.

5. Simulation and discussion

To show the performance obtained by the proposed control scheme of WECS based on BDFIG with OTC-MPPT, various numerical simulations were carried out a 2.5 kW BDFIG. The following simulations were carried out under MATLAB/SIMULINK (R 2018a) environment.

All the BDFIG parameters used in the simulations are given in the Table 1.

Table 1. The parameters employed in the simulations

BDFIG	**WIND TURBINE**
P = 2.5 kW. $P_p = 3,\ P_c = 1.$ $R_p = 1.732\ \Omega,$ $R_c = 1.079\Omega,$ $R_r = 0.473\ \Omega.$ $L_p = 714.8$ mH $L_c = 121.7$ mH $L_r = 132.6$ mH $M_p = 242.1$mH $M_c = 59.8$ mH J = 0.053 $Kg \cdot m^2$ F = 0.003 $N \cdot ms / rd$	R = 5m J = 61 $Kg \cdot m^2$ F = 0.01 $N \cdot ms / rd$ G = 20 $c_{p-opt} = 0.5$ $\lambda_{opt} = 9.14$

The obtained curve illustrates in Figure 4 that if the wind profile varies, c_p can rapidly reach around the optimal value. The optimum value of the power coefficient is selected, that is $c_{p-\max} = 0.5$

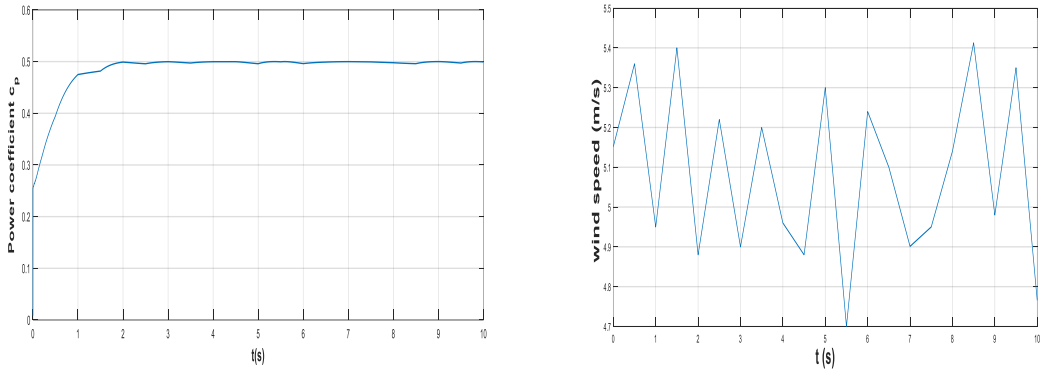

Figure 4. Power coefficient c_p and wind speed

From the obtained results illustrated in Figure 5, it can be seen that even in the case of a very variable system, the electromagnetic torque of the BDFIM will effectively follow the reference torque provided by the OTC-MPPT scheme The BDFIM speed follows the wind speed closely to keep λ constant, which indicates that the system works with optimal power. This verifies the decoupling between the electromagnetic torque and reactive powers.

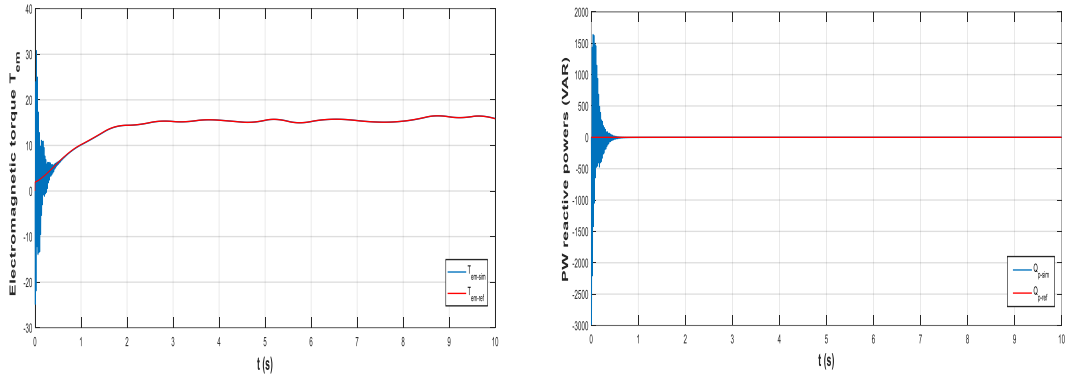

Figure 5. The electromagnetic torque and PW reactive powers

Figure 6 and Figure 7 illustrate the temporal evolution of the PW currents i_{dp} and i_{qp} and of the CW currents i_{dc} and i_{qc}, respectively. These currents can increase or decrease depending on the wind conditions.

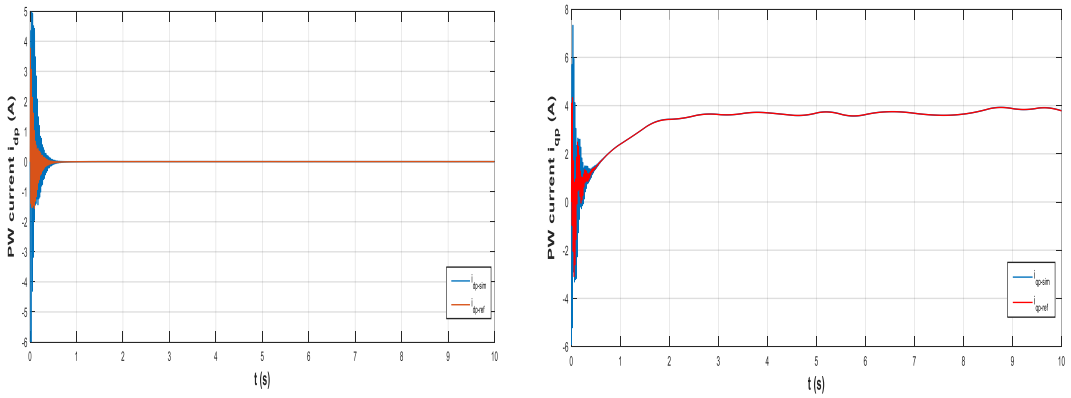

Figure 6. d-q PW current

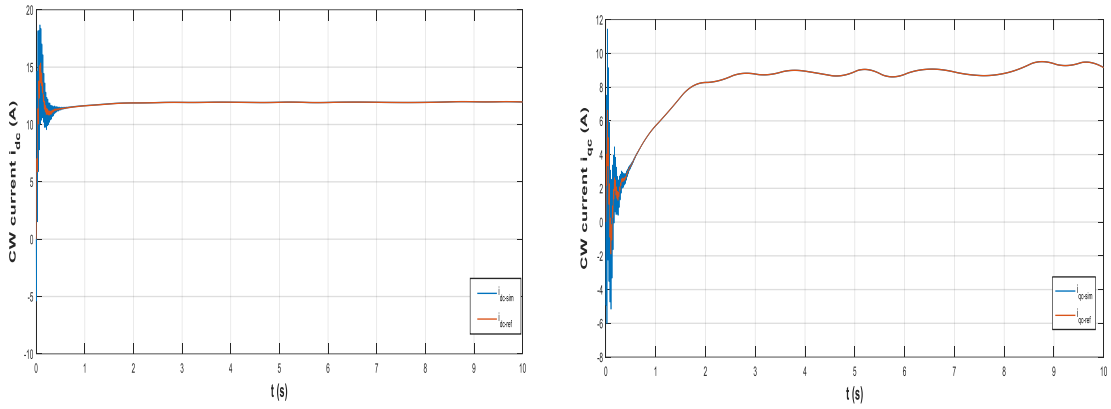

Figure 7. d-q CW current

Figure 8 illustrates the temporal evolution of the stator phase currents i_{abc} of PW. It should be noted that these currents have a constant frequency regardless the operating regime.

Figure 9 shows the temporal evolution of the phase currents i_{abc} of CW. It can be observed that these currents have a variable frequency which changes with the speed of rotation.

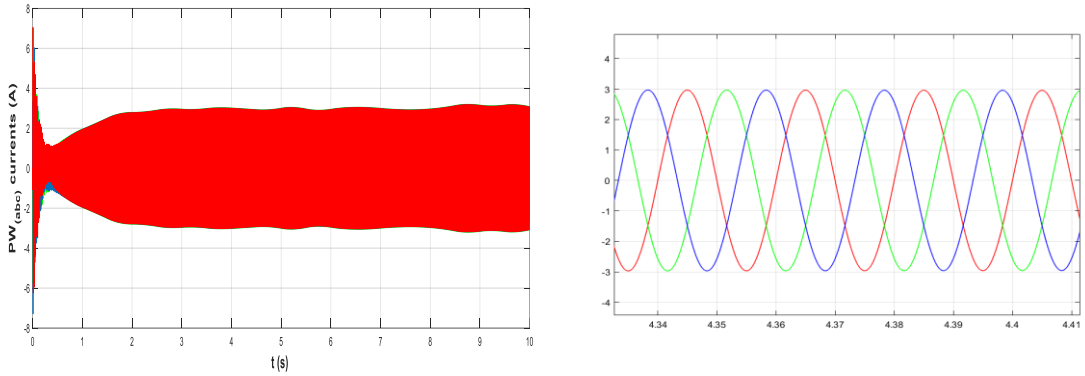

Figure 8. $PW_{(abc)}$ currents

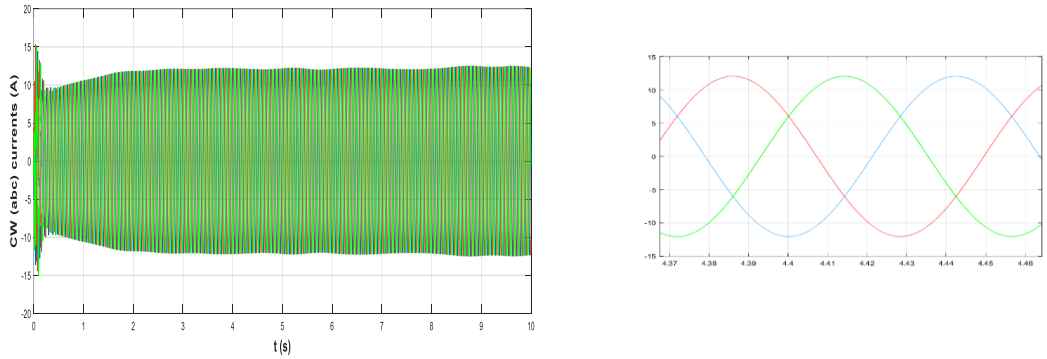

Figure 9. $CW_{(abc)}$ currents

6. Conclusion

This study presents the vector control of a brushless dual-fed asynchronous machine incorporated in a WECS which is driven by OTC-MPPT. To reduce the costs of of the control scheme and guarantee that the generator works at maximum power with weak oscillations, in addition to keep up with the wind speed variation with the optimal λ and the maximal c_p an OTC-based MPPT scheme was proposed. The main feature of the OTC-MPPT scheme is that there is no need to use wind s peed sensors.

The simulation results prove the validity of the suggested control scheme and the advantage of working with OTC-based MPPT to allow the wind turbine to operate at its optimum power over a wide range of wind speeds even in the context of highly variable wind speeds without mechanical sensor.

Future work may focus on the following: a) On the other hand to overcome the problem of using the tuning PI controller parameters. The aim is to apply advanced optimization algorithm such the BAT algorithm, and the Grasshopper optimization algorithm (GOA), which allow one to obtain the optimal parameter values for controllers and consequently improve the performance of a control system. b) In addition, to guarantee constant power generation and to ensure the functions of the wind energy conversion system (voltage regulation, frequency regulation...), the aim is to introduce an intelligent flywheel energy storage system based on a permanent magnet synchronous machine (PMSM) in the proposed wind generator system.

List of symbols

V	Wind speed (m/s)
ρ	Air density, kg/m^3
s	Surface area swept by the blade, m^2
p_T	Mechanical power of the turbine Watts
T_m	Mechanical torque of the turbine
Ω_{mec}	Mechanical speed of the rotor, rad/s
ω_p and ω_c	Power winding angular frequency and control winding angular frequency
ω_r	Synchronous rotor speed
P_p	Active power of the power winding Watts
Q_p	Reactive power of the power winding Var
V_{dp}, V_{qp}, V_{dc} and V_{qc}	Components of the power winding voltage and the control winding voltage respectively
V_{dr} and V_{qr}	Components of the rotor winding voltage
ψ_{dp}, ψ_{qp}, ψ_{dc} and ψ_{qc}	Components of the power winding flux and control winding flux respectively
ψ_{dr} and ψ_{qr}	Components of rotor winding flux
i_{dp}, i_{qp}, i_{dc} and i_{qc}	Components of the power winding current and control winding current respectively
i_{dr} and i_{qr}	Components of rotor winding current
R_P, R_c and R_r	Power winding resistance, control winding Resistance and rotor winding Resistance respectively

M_P	Mutual inductance between Power winding and rotor
M_c	Mutual inductance Control winding and rotor
L_p , L_c and L_r	Power winding inductance, Control winding inductance and rotor inductance respectively
$v_c^{\alpha\beta}$	The tension in the clarke Transformation

REFERENCES

1. Aicha, A., Youcef, M., Said, H. & Tayeb, A. (2019). *Intelligent maximum power tracking control of a PMSG wind energy conversion system*. Asian Journal of Control 21(4) 1980-1990. DOI: 10.1109/ICEE-B.2017.8191990.
2. Bouras, M. & Kouzi, K. (2017). *Analysis of Novel Flywheel Energy Storage System Based on Dual Stator Induction Machine Incorporated in Wind Energy Systems Using Intelligent Approach*. In intenational Conference in Artificial Intelligence in Renewable Energetic Systems (357-365). Springer, Cham. DOI: 10.1007/978-3-319-73192-6_37.
3. Eltamaly, A. M. & Farh, H. M. (2013). *Maximum power extraction from wind energe system based on fuzzy logic control*. Electric Power Systems Research, 97, 144-150. DOI: 10.1016/j.epsr.2013.01.001.
4. Li, Q. & Pan, Z. P. (2001). *The modeling and simulation of brushless doubly-fed generator of wind power generation system*. In 4th IEEE International Conference on power Electronics and Drive Systems IEEE PEDS 2001-Indonesia. Proceedings (Cat. No. 01TH85940), Vol. 2, pp. 811-814. IEEE. DOI: 10.1109/PEDS.2001.975423.
5. Lobo, F. J. P. (2003). *Commande de la BDFM. Modélisation, conception et commande d'une machine asynchrone sans balais doublement alimentée pour la génération à vitesse variable (Doctoral dissertation)*. Institut National Polytechnique de Grenoble-INPG.
6. Perelmuter, V. (2016). *Renewable Energy Systems: Simulation with Simulink® and SimPowerSystems™*. CRC Press.
7. Rahab, A., Senani, F. & Benalla, H. (2017). *Direct power control of brushless doubly-fed induction generator used in wind energy conversion system*. International Journal of Power Electronics and Drive System (IJPEDS), 8(1), 417-433.
8. Serhoud, H. & Benattous, D. (2013). *Simulation of grid connection and maximum power point tracking control of brushless doubly-fed generator in wind power system*. Frontiers in Energy 7(3), 380-387. DOI: 10.1007/s11708-013-0252-z.
9. Tir, Z. & Abdessemed, R. (2014). *Control of a wind energy conversion system based on brushless doubly fed induction generator*. Revue des Énergies Renouvelables, 17(1). 55-69.
10. Trejos-Grisales, L., Duarnizo-Lemus, C. & Serna, S. (2014). *Overall description of wind power systems*. Ingeniería y Ciencia, 10(19), 99-126. DOI: 10.17230/ingciencia.10.19.5.
11. Tria, F. & Ben Attous, D. (2012). *Simulation for strategy of Maximal Wind energy capture of doubly fed induction generators*. International Journal of Chemical and Pertroleum Sciences 1(1), 17-26.
12. Zhou, D., Spee, R. & Alexander, G. C. (1997). *Experimental evaluation of a rotor flux oriented control algorithm for brushless doubly-fed machines*. IEEE Transactions on Power Electronics, 12(1), 72-78. DOI: 10.1109/63.554171.

Mohamed HAMIDAT obtained his Master`s degree in Electromechanics in 2019 at the University of Laghouat in Algeria. He is a PhD Student in the field of Electrical Control. His research focuses on Advanced Control of Electrical Machines, Intelligent Artificial Control, Optimization, Renewable Energy Systems Control, and Electrical Storage Systems.

Katia KOUZI was born in Algeria. She obtained her Bachelor degree in 1998 and later her Master's degree in Electrical Engineering 2002, respectively. She received her PhD degree in Electrical and Computer Engineering from the University of Batna in 2008. Her research interests focus on Advanced Control of AC Drives, including Vector, Sensorless, and Intelligent Artificial Control, Electric vehicles (EVs) control Renewable Energy Control Systems, Management and Storage Systems. She is a researcher at the Laboratoire Matériaux, Systèmes Énergétiques, Energies Renouvelables et Gestion de l'Énergie (LMSEERGE) as well as a full-time professor at the Electrical Engineering Institute at the University of Laghouat in Algeria.